Piezoelectricity in two dimensions: Graphene vs. molybdenum disulfide

Xiaoxue Song, Fei Hui, Theresia Knobloch, Bingru Wang, Zhongchao Fan, Tibor Grasser, Xu Jing, Yuanyuan Shi, and Mario Lanza

Citation: Appl. Phys. Lett. **111**, 083107 (2017); doi: 10.1063/1.5000496
View online: http://dx.doi.org/10.1063/1.5000496
View Table of Contents: http://aip.scitation.org/toc/apl/111/8
Published by the American Institute of Physics

Piezoelectricity in two dimensions: Graphene vs. molybdenum disulfide

Xiaoxue Song,[1] Fei Hui,[1] Theresia Knobloch,[1,2] Bingru Wang,[1] Zhongchao Fan,[3,4] Tibor Grasser,[2] Xu Jing,[1] Yuanyuan Shi,[1] and Mario Lanza[1,a)]
[1]*Institute of Functional Nano and Soft Materials, Collaborative Innovation Center of Suzhou Nanoscience and Technology, Jiangsu Key Laboratory for Carbon-Based Functional Materials and Devices, Soochow University, 199 Ren-Ai Road, Suzhou 215123, China*
[2]*Institute of Microelectronics, TU Wien, Gusshausstrasse 27-29, 1040 Vienna, Austria*
[3]*Engineering Research Center for Semiconductor Integrated Technology, Institute of Semiconductors, Chinese Academy of Sciences, Beijing 100083, China*
[4]*School of Electronic, Electrical and Communication Engineering, University of Chinese Academy of Sciences, Beijing 101408, China*

(Received 8 March 2017; accepted 16 August 2017; published online 25 August 2017)

The synthesis of piezoelectric two-dimensional (2D) materials is very attractive for implementing advanced energy harvesters and transducers, as these materials provide enormously large areas for the exploitation of the piezoelectric effect. Among all 2D materials, molybdenum disulfide (MoS_2) has shown the largest piezoelectric activity. However, all research papers in this field studied just a single material, and this may raise concerns because different setups could provide different values depending on experimental parameters (e.g., probes used and areas analyzed). By using conductive atomic force microscopy, here we *in situ* demonstrate that the piezoelectric currents generated in MoS_2 are gigantic (65 mA/cm^2), while the same experiments in graphene just showed noise currents. These results provide the most reliable comparison yet reported on the piezoelectric effect in graphene and MoS_2. *Published by AIP Publishing.* [http://dx.doi.org/10.1063/1.5000496]

With the rise of low dimensional materials [e.g., nanowires, fullerenes, and two dimensional (2D) sheets], energy harvesters and transducers have experienced a transformation in terms of size, architecture, and performance.[1] Among them, applications based on the piezoelectric effect (conversion of mechanical energy into electrical energy and vice versa) are especially attractive because low dimensional materials can provide a large surface area for potential generation.[2] The synthesis of piezoelectric 2D materials would represent a huge milestone towards the realization of this technology. In these materials, a mechanical strain can break the bonding symmetry, producing a potential difference between two points of the 2D sheet. Then, if a load resistor is connected, current can be generated.

The piezoelectric effect in 2D materials was initially studied via theoretical calculations. Graphene (carbon atoms arranged in a sp^2 hexagonal lattice) does not show a piezoelectric effect intrinsically.[3] In Ref. 4, it was suggested that by doping one surface of the graphene sheet with different species (e.g., Li, K, H, or F), small piezoelectric potentials could be generated in the normal plane. Hexagonal boron nitride (*h*-BN) showed a piezoelectric effect when strain is applied in plane.[5] In this case, the combination of two different atomic elements (N and B) is a key element for producing the asymmetry in the 2D sheet. Recent works predicted that the 3-layered structure of transition metal dichalcogenides may provide a genuine framework for symmetry breakdown, which should result in a superior piezoelectric effect. References 6 and 7 empirically demonstrated the piezoelectric effect in MoS_2 at the device level, and References 8–10 performed nanoscale experiments to determine the piezoresistive effect (variation of resistivity with the strain) but not generation of current in the absence of bias). Nevertheless, in all these cases, the magnitude of the currents generated when straining different materials was not compared using the same setup.

In this work, we present an *in situ* characterization of piezoelectricity in graphene and MoS_2 using the same setup, allowing us to rigorously evaluate the differences. Our conductive atomic force microscopy (CAFM) measurements confirm that graphene sheets exposed to mechanical strains do not produce piezoelectric currents. On the contrary, similar experiments conducted on MoS_2 showed gigantic current densities of 65 mA/cm^2 without the need of bias application. The characterization of both materials with the same setup is more reliable than the demonstrations previously reported and invariably proves the presence of piezoelectricity in MoS_2.

The piezoelectric effect in graphene and MoS_2 has been studied at the nanoscale via CAFM. The 2D sheets were transferred on a Si substrate containing holes with diameters ranging between 1.5 and 6 μm (patterned via reactive ion etching). Then, the conductive tip of the CAFM was used to push the suspended membrane down inside the hole, while the current was simultaneously monitored. The goal of these experiments was to observe if the mechanical strain applied to the 2D material produced any signal of current generation (without applying bias).

The graphene single layer (GSL) sheets were grown via chemical vapor deposition (CVD) on Cu foils at the laboratories of Hangzhou Gelanfeng Nano Technology.[11,12] The graphene sheets were transferred onto the perforated Si substrate with the assistance of a polymethyl methacrylate (PMMA) scaffold.[13] A 100–200 nm thick PMMA layer was

a)Author to whom correspondence should be addressed: mlanza@suda.edu.cn

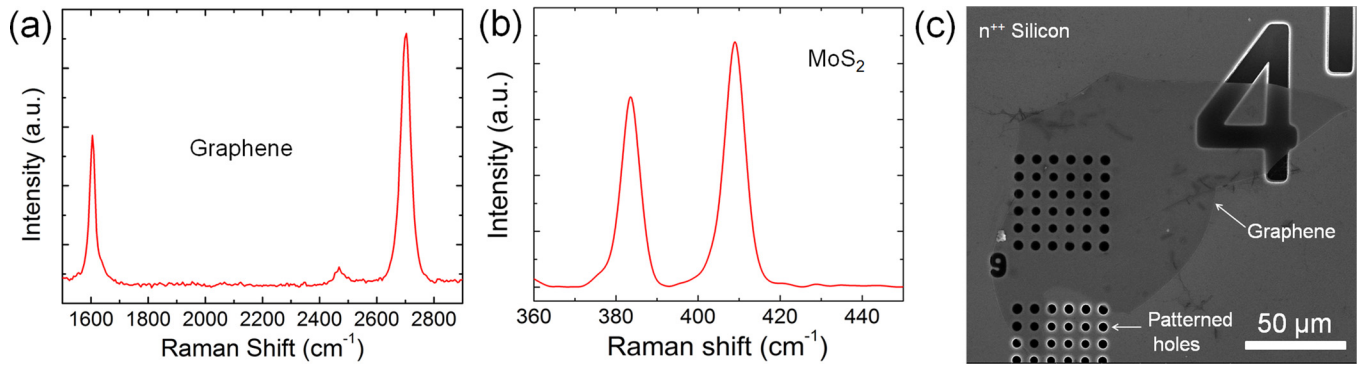

FIG. 1. Raman spectrum of (a) GSL and (b) multilayer MoS_2. (c) SEM image of the Si substrate patterned with holes and partly covered by a GSL sheet.

deposited on the GSL/Cu samples using a spinner (2000 rpm for 1 min), followed by a soft baking at 170 °C for 5 min. Then, the Cu foil was etched in a $FeCl_3$ bath. The PMMA/GSL stack was cleaned with hydrochloric acid (HCl) for 5 s and rinsed with pure water. Finally, the PMMA/GSL stack was retrieved using the perforated Si substrate, and the PMMA scaffold was removed in an acetone bath.[13,14] The transfer experiments were carried out in a fume hood at room temperature (~25 °C).

The MoS_2 sheets were fabricated via liquid phase exfoliation (LPE). More specifically, 4 mg of MoS_2 powder (Alfa Aesar) were diluted in 10 mL isopropyl alcohol (IPA) using a tube probe, which was immersed in an ultrasonic bath (KQ-100KDB High Power NC, Kunshan Ultrasonic Instruments) for 26 h at a power of 90 W. The thin flakes and the larger particles were separated by centrifugation (H1650-W centrifuge from Cence Instrument) at 4000 rpm for 15 min. Finally, the supernatant consisting of ultra-thin MoS_2 flakes was picked using a pipette and one drop was deposited on the perforated Si substrate. After drying (in natural conditions), the MoS_2 sheets remained suspended on the holes.

The quality of the graphene and MoS_2 sheets was evaluated using a Raman spectrometer in a backscattering configuration (model LabRAMHR800). The excitation was provided by an Ar laser ($\lambda = 514$ nm), as in References 15 and 16. In order to improve the Raman peak signal, this specific experiment was performed by transferring the 2D sheets on 300 nm SiO_2/Si wafers.[15,16] Additionally, the presence of the graphene and MoS_2 sheets suspended on the substrate was verified using a Zeiss SUPRA55 Scanning Electron Microscope (SEM). The morphology and the piezoelectric effect of the 2D materials were analyzed with a Veeco Multimode V AFM. Pt-Ir varnished silicon tips from Bruker (model SCM-PIC, item no. A009/07-07/14) have been employed.

Figure 1(a) shows the Raman spectrum of the GSL samples. The G peak at 1600 cm^{-1} is related to the doubly degenerated zone center E_{2g} mode, and the G′ peak at 2700 cm^{-1} is emitted from a second-order process involving zone-boundary phonons.[17,18] This proves that the GSL sheets grown by CVD are monolayers.[19] The Raman spectrum in Fig. 1(b) shows the two typical features of MoS_2 at 383 cm^{-1} and at 409 cm^{-1}, corresponding to the E^1_{2g} and A_{1g} modes (respectively).[20] Both of them are first order Raman modes, where the E^1_{2g} mode is similar to the E_{2g} mode in graphene, as it involves an in-plane vibration of the molybdenum sublattice against the sublattice formed by the sulphur atoms. On the contrary, the A_{1g} mode exists only in MoS_2, as it corresponds to out-of-plane vibrations of the upper and lower sublattices of sulphur atoms against each other.[18] The position and height of the Raman peaks in Fig. 1(b) indicate that the MoS_2 sheet is a multilayer.[21] Figure 1(c) shows the SEM picture of a perforated Si substrate partially covered with a GSL sheet.

In the next step, we focus on one GSL-covered hole from Fig. 1(c). Zoom-in SEM pictures [see Fig. 2(a)] prove the presence of suspended GSL on the hole. Even some wrinkles can be spotted, corroborating the continuous nature of the GSL sheet. Figure 2(b) shows the topography map (measured in the tapping mode); the wrinkles can be again easily observed. The deep area inside the hole [black area in Fig. 2(b)] shows a depth almost constant at ~180 nm [see the inserted cross section in Fig. 2(b)]. This high value can be explained by considering that the graphene sample has been

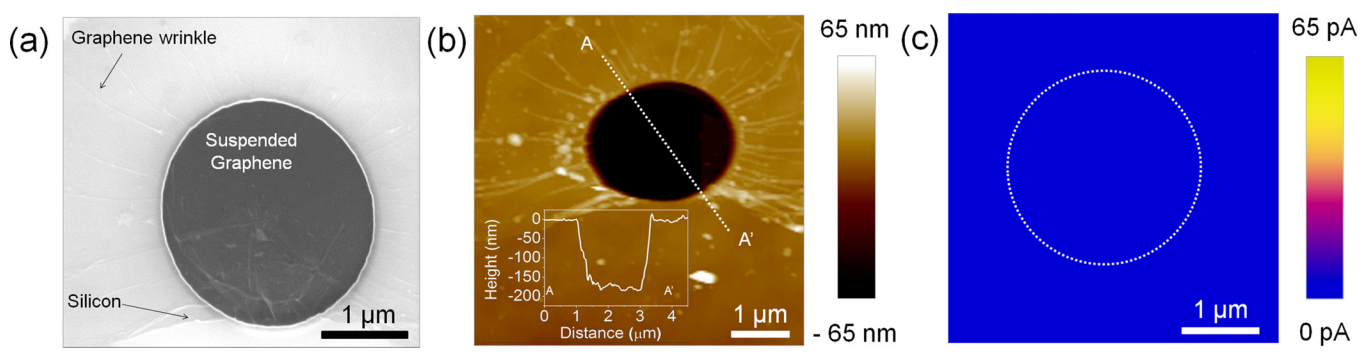

FIG. 2. (a) SEM and (b) topographic AFM images of the hole covered with graphene. The inset in (b) shows the A-A′ cross section. (c) AFM current map measured with zero bias, showing the absence of current in the graphene sheet.

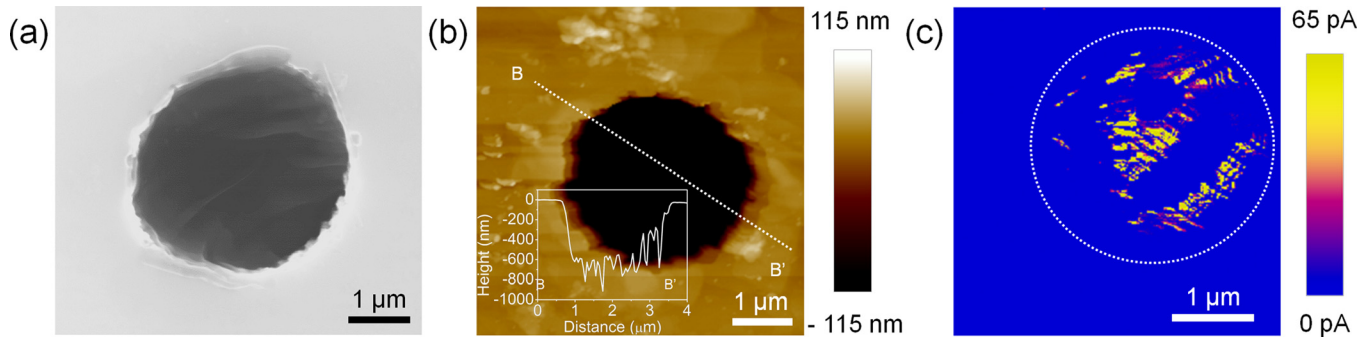

FIG. 3. (a) SEM and (b) topographic AFM images of the hole covered with MoS_2. The inset in (b) shows the A-A′ cross section. (c) AFM current map measured with zero bias, showing the generation of abundant currents in the MoS_2 sheet.

stretched by the force applied through the AFM tip during the scan. The same hole has been scanned again, this time in the contact mode (without any bias applied), and the current scan has been collected [Fig. 2(c)]. The area corresponding to the hole has been highlighted with a dashed white circle. As can be seen, when using a Z-axis scale bar of 65 pA no currents can be observed. When the Z-axis scale bar is set to 1 pA (see Fig. S1 in the supplementary material), only very small currents similar to the electrical noise can be observed. In that case, it should be highlighted that: (i) the currents outside and inside the hole are similar, indicating that the pressure of the tip did not produce any effect; and (ii) the slight accumulation of current in the central part is too small to be considered as the current generation, and conversely it might be related to an increase in the contact area between the tip and the 2D membrane when pushed in the center.

The SEM, AFM, and CAFM experiments have been repeated on the suspended MoS_2 sheets. The SEM images [Fig. 3(a)] corroborate the presence of MoS_2 on the holes. The topographic maps collected on the suspended MoS_2 sheet are displayed in Fig. 3(b). The areas with different colors are related to the depth of the hole. From the cross section of the topographic map [see inset in Fig. 3(b)], it can be observed that the maximum depth the MoS_2 deflected is ~800 nm. Figure 3(c) shows the current map collected on the MoS_2 sheet in the absence of bias. Abundant (~65 pA) currents in the absence of bias have been rapidly detected. As the tip/sample contact area is of the order of ~100 nm^2,[22] the values in Fig. 3(c) represent current densities above 65 A/cm^2. Because other reports in this field did not use the same setup (e.g., References 8–10 measure the current horizontally using patterned electrodes while applying a vertical strain), no direct current comparison is allowed. Nevertheless, the presence of such large currents without applying any bias [Fig. 3(c)] and the absence of currents outside the hole corroborate that the currents generated are related to the mechanical strain applied to the MoS_2 sheet. Interestingly, some conductive areas in Fig. 3(c) are separated by non-conductive regions; this indicates the presence of step-like thickness fluctuations in the MoS_2 sheet, as it is known that odd and even amounts of layers can produce very different piezoelectric responses.[6]

The experiments presented in Fig. 3 have been repeated using different contact forces, which are controlled by changing the parameter called deflection setpoint (DS) in the CAFM software. Topographic maps collected at higher contact forces produced a larger deflection of the MoS_2 sheet, resulting in a larger mechanical strain in the 2D sheet. This result is displayed in Fig. S2 in the supplementary material, which shows the cross section of the topographic maps for different DSs. As it can be observed, the deflection of the MoS_2 sheet is proportional to the applied force (DS). The simultaneously collected current maps reveal an increase of current with the contact force (see Fig. S3 in the supplementary material). This result is also displayed in Fig. S2b (supplementary material) by plotting the cross sections of the current maps at different DSs. Overall, the CAFM tests at different contact forces confirm the strong relation between mechanical strain and currents measured, which is characteristic of the piezoelectric effect. These experiments are highly reproducible, and they have been corroborated in 8 different graphene-covered holes and 20 different MoS_2-covered holes.

Finally, it should be highlighted that high strains applied to MoS_2 sheets may produce semiconductor-to-metal transition, but this phenomenon is not behind the currents we observe because: (i) such transition takes place at pressures above 10 GPa,[23] while the maximum pressure we are applying in our CAFM experiments is always below 2.47 GPa; and (ii) there is no bias applied in these experiments, i.e., even a semiconductor-to-metal transition would not produce currents. Furthermore, according to Ref. 24, the flexoelectric effect in MoS_2 is negligible, and therefore, we discarded it.

In conclusion, the presence of piezoelectricity in both graphene and MoS_2 has been investigated via CAFM, using exactly the same setup. This is important for comparing the effect in both materials, as the values from different papers may be misleading due to setup differences. The comparison of the piezoelectric properties of different 2D materials using the same setup (irrespective if at the device level or at the nanoscale) has never been reported before. Our measurements indicate that, while the currents measured when stretching GSL sheets are negligible, mechanical strains in MoS_2 sheets produce abundant piezoelectricity (currents up to 65 mA/cm^2). The currents generated in the MoS_2 sheet increase with the mechanical strain applied. These results corroborate *in situ* the different piezoelectric ability of graphene and MoS_2, and position MoS_2 as a firm candidate for future 2D energy harvesting.

See supplementary material for additional CAFM current images with different scales and the correlation between the contact force and the registered piezoelectric currents generated are presented.

This work was supported by the Young 1000 Global Talent Recruitment Program of the Ministry of Education of China, the National Natural Science Foundation of China (Grant Nos. 61502326, 41550110223, and 11661131002), the Jiangsu Government (Grant No. BK20150343), the Ministry of Finance of China (Grant No. SX21400213), and the Young 973 National Program of the Chinese Ministry of Science and Technology (Grant No. 2015CB932700), as well as by the Austrian Science Fund (FWF) Grant No. I 2606-N30. The Collaborative Innovation Center of Suzhou Nano Science and Technology, the Jiangsu Key Laboratory for Carbon-Based Functional Materials and Devices, the Priority Academic Program Development of Jiangsu Higher Education Institutions, the 111 Project from the State Administration of Foreign Experts Affairs, and the Opening Project of Key Laboratory of Microelectronic Devices and Integrated Technology (Institute of Microelectronics, Chinese Academy of Sciences) are also acknowledged. The authors acknowledge the help from Professor Guangyin Jing from Northwest University.

[1]H. A. Sodano, D. J. Inman, and G. Park, J. Intell. Mater. Syst. Struct. **16**, 799 (2005).
[2]C. N. R. Rao, K. Gopalakrishnan, and U. Maitra, ACS Appl. Mater. Interfaces **7**, 7809 (2015).
[3]S. Chandratre and P. Sharma, Appl. Phys. Lett. **100**, 023114 (2012).
[4]M. T. Ong and E. J. Reed, ACS Nano **6**(2), 1387 (2012).
[5]K. H. Michel and B. Verberck, Phys. Rev. B **83**(11), 115328 (2011).
[6]W. Wu, L. Wang, Y. L. Li, F. Zhang, L. Lin, S. Niu, D. Chenet, X. Zhang, Y. Hao, T. F. Heinz, J. Hone, and Z. L. Wang, Nature **514**, 470 (2014).
[7]S. K. Kim, R. Bhatia, T. H. Kim, D. Seol, J. H. Kim, and H. Kim, Nano Energy **22**, 483 (2016).
[8]J. J. Qi, Y. W. Lan, A. Z. Stieg, J. H. Chen, Y. L. Zhong, L. J. Li, C. D. Chen, Y. Zhang, and K. L. Wang, Nat. Commun. **6**, 7430 (2015).
[9]H. Y. Zhu, Y. Wang, J. Xiao, M. Liu, S. M. Xiong, Z. J. Wong, Z. L. Ye, Y. Ye, X. B. Yin, and X. Zhang, Nat. Nanotechnol. **10**, 151 (2015).
[10]S. Manzeli, A. Allain, A. Ghadimi, and A. Kis, Nano Lett. **15**, 5330 (2015).
[11]K. S. Kim, Y. Zhao, H. Jang, S. Y. Lee, J. M. Kim, K. S. Kim, J.-H. Ahn, P. Kim, J.-Y. Choi, and B. H. Hong, Nature **457**, 706 (2009).
[12]X. Li, W. Cai, J. An, S. Kim, J. Nah, D. Yang, R. Piner, A. Velamakanni, I. Jung, E. Tutuc, S. K. Banerjee, L. Colombo, and R. S. Ruoff, Science **324**, 1312 (2009).
[13]J. W. Suk, A. Kitt, C. W. Magnuson, Y. Hao, S. Ahmed, J. An, and A. K. Swan, ACS Nano **5**, 6916 (2011).
[14]W. Regan, N. Alem, B. Aleman, B. Geng, C. Girit, L. Maserati, F. Wang, M. Crommie, and A. Zettl, Appl. Phys. Lett. **96**, 113102 (2010).
[15]A. Castellanos-Gomez, M. Barkelid, A. M. Goossens, V. E. Calado, H. S. J. van der Zant, and G. A. Steele, Nano Lett. **12**, 3187 (2012).
[16]M. Buscema, M. Barkelid, V. Zwiller, H. S. J. van der Zant, and G. A. Steele, Nano Lett. **13**, 358 (2013).
[17]A. C. Ferrari, J. C. Meyer, V. Scardaci, C. Casiraghi, M. Lazzeri, F. Mauri, S. Piscanec, D. Jiang, K. S. Novoselov, and S. Roth, Phys. Rev. Lett. **97**, 187401 (2006).
[18]M. A. Pimenta, E. del Corro, B. R. Carvalho, C. Fantini, and L. M. Malard, Acc. Chem. Res. **48**, 41 (2015).
[19]Y. Y. Wang, Z. H. Ni, T. Yu, Z. X. Shen, H. M. Wang, and Y. H. Wu, J. Phys. Chem. C **112**(29), 10637 (2008).
[20]S. Z. Butler, S. M. Hollen, L. Y. Cao, Y. Cui, J. A. Gupta, H. R. Gutierrez, T. F. Heinz, S. S. Hong, J. X. Huang, A. F. Ismach, E. Johnston-Halperin, M. Kuno, V. V. Plashnitsa, R. D. Robinson, R. S. Ruoff, S. Salahuddin, J. Shan, L. Shi, M. G. Spencer, M. Terrones, W. Windl, and J. E. Goldberger, ACS Nano **7**, 2898 (2013).
[21]C. Lee, H. Yan, L. E. Brus, T. F. Heinz, J. Hone, and S. Ryu, ACS Nano **4**(5), 2695 (2010).
[22]M. Lanza, M. Reguant, G. Zou, P. Lv, H. Li, and R. Chin, Adv. Mater. Interfaces **1**(5), 1300101 (2014).
[23]A. P. Nayak, S. Bhattacharyya, J. Zhu, J. Liu, X. Wu, T. Pandey, C. Jin, A. K. Singh, D. Akinwande, and J. F. Lin, Nat. Commun. **5**, 3731 (2014).
[24]J. Zhang, C. Wang, and C. Bowen, Nanoscale **6**(22), 13314 (2014).